3D magnetotelluric inversion reveals the superposition of tectonic systems in the northern Songliao Basin

Tianqi Wang[1], Guoqing Ma[1,2], Jiangtao Han[1,2*], Wenyu Liu[3], Zikun Zhou[1], and Jianqiang Kang[1]

[1]College of Geoexploration Science and Technology, Jilin University, Changchun, China.

[2]Key Laboratory of Applied Geophysics, Changchun, China.

[3]School of Geophysics and Measurement-Control Technology, East China University of Technology, Nanchang, China.

Corresponding author: Jiangtao Han (hanjt@jlu.edu.cn)

Key Points:

- 3D modeling of Songliao Basin via magnetotelluric array dataset
- Discovering conductor in the northern Songliao Basin hints at the extreme point of lithospheric thinning
- The superposition of tectonic systems is responsible for the current crust-mantle structure.

Abstract

The creation and evolution of the Songliao Basin is closely related to the closure of the Paleo-Asian Ocean and the Mongolia-Okhotsk Ocean, and the subduction of the Paleo-Pacific Ocean. In an attempt to demonstrate the various attributes of the lithospheric structure under structural superimposition and transformation of the Songliao Basin, this work used full impedance 3D inversion to obtain a 3D electrical structural model of the northern Songliao Basin for the first time. The results showed there are NE-trending high-resistance anomalies and sporadic low-resistance anomalies at the depth of less than 10 km. At 15-30 km, there are several NE- and NW-trending high-conductivity anomalies and there is a large area of SN-oriented high conductor at 50 km. The outcomes of the investigation demonstrate: 1) The high-resistance anomalies found in the NE direction of the upper crust are consistent with the position of the volcanic rocks predicted by the reflection earthquake, whereas the low-resistance anomalies correspond to the distribution of shallow faults and rifts. They constitute the main components of the upper crust of the Songliao Basin; 2) The high conductivity anomalies occurring at the intersection of the central depression zone and the north plunge zone represent the thinnest position of the lithosphere in the Songliao Basin; 3) The high-conductor anomalies in crust-mantle can be attributed to the paleo-shear zones which were generated in the collage of micro-continents during the Paleo-Asian Ocean closure, and reactivated under the continuous transformation of the Mongolia-Okhotsk and the Paleo-Pacific tectonic systems in the later period.

1 Introduction

The Songliao Basin is a large Mesozoic-Cenozoic sedimentary basin, superimposed on the Paleozoic basement and located in northeastern China. The precise location of the Songaliao Basin is the eastern section of the Central Asian Orogenic Belt (CAOB). The main body of the regional structure is in the Songnen Block which lies adjacent to the Xing'an block, by the Nenjiang fault in the west and connected with the Jiamusi block in the east by the Yilan-Yitong fault. The dynamic background of Songliao Basin's is relatively complicated, as it is located at the intersection of multiple periods of structural systems. During the Paleozoic era, the Songliao Basin experienced the evolution of the Paleo-Asian ocean tectonic system. With the closure of the Paleo-Asian ocean, many micro-continent blocks in the Northeast (E'ergun block, Xing'an block, Songnen block, Zhangguangcailing block, Jiamusi block, and Xingkai Block) were combined into a composite land block (Xiao et al., 2003; Miao et al., 2008; Jian et al., 2008). During the Mesozoic, the "scissor" closure of Mongolia Okhotsk Ocean from west to East and the westward subduction of the Paleo-Pacific slab placed the Songliao Basin under the combined action of these two dynamic systems (Xu et al., 2009; Wu et al., 2011).

The dynamic yet complicated background restricts the formation and evolution of magmatism, stratigraphic deposits, and structural frameworks of the Songliao Basin. The closure and extinction of the Paleo-Asian Ocean and the Mongolia-Okhotsk Ocean, and the westward

subduction of the Paleo-Pacific Ocean left a widespread of granite along the Solon-Xar Moron River-Changchun area, towards the west of the Da Hingan Mountains, and east of the Korean Peninsula-Songliao Basin (Wang et al., 2017). Under the action of different structural systems, there are regional unconformities at the top of the Yingcheng Formation and Nenjiang Formation in the Songliao Basin as well as their upper and lower structural frameworks, hence the stratigraphic distribution and direction, and rock combinations are significantly different (Wang et al., 2007). Zircon U-Pb age statistics of volcanic rocks revealed that there were multiple periods of volcanic activity in the Songliao Basin during the Mesozoic era. Volcanic rocks of different periods recorded the process of transition from the Mongolia-Okhotsk tectonic domain to the Pacific tectonic domain. (Xu et al., 2013). Under the joint action of the Mongolia-Okhotsk tectonic system and the Pacific tectonic system, the hydrocarbon seismic stack section in the Binbei area of the Songliao Basin presents a thrust nappe fault system having a two-way form, showing uneven strength longitudinally and laterally (Shan et al., 2009). Various phenomena indicate that the current structural morphology of the Songliao Basin is a result of the joint action of different structural systems. Although there is a continuous superimposition of late structural systems the traces of pre-existing structural systems can still be observed from various angles.

Besides, the subduction of the Pacific plate into Eurasia resulted in the thinning of the lithosphere in eastern China (Wu et al., 2005; Tao et al., 2014; Zhang et al., 2014). Thus, in comparison to the Da Hingan Mountains and Zhangguangcai Mountains flanking on both sides, the depth of lithospheric mantle bottom interface of Songliao Basin is as thin as 60-100 km (Wang et al., 2016; He and Santosh, 2016; Han et al., 2018). The maximum geothermal gradient is 62℃/km (Liu et al., 2017). The thinning of the lithosphere is accompanied by crustal thinning to a considerable extent. The seismic profile revealed that the depth of the Moho in the Songliao Basin is 29~38 km (Yang et al., 2003; Wang et al., 2016). The shallowest position is on the Mingshui-Anda-Changling line, and the variation characteristics show a trend of gradually getting deeper from the middle to the east and west sides.

Detection and imaging of complex and deep processes that take place in the lithosphere by the effect of fluids are carried out by the Magnetotagnetic field (MT). Such detection is possible by the magnetotactic field is possible because resistivity is essentially a transmission property of the medium and is particularly sensitive to the presence of low resistivity phases of interconnections, such as partial melts or aqueous fluids (Wei et al., 2001; Wannamaker et al., 2008). With the rapid development of 3D magnetotelluric inversion (Siripunvaraporn et al., 2005; Egbert and Kelbert, 2012), it has been used and is playing a major role in the study of the basin’s structure (Peacock et al., 2015; Zeng et al., 2015) and volcanic mechanism (Heise et al., 2008; Aizawa et al., 2014; Zhang et al., 2016; Li et al., 2020). Earlier MT studies in this area were mostly conducted on isolated profiles, thus making it difficult to conduct a comprehensive study of large structures. There is, however, still a major lack of high-resolution electrical evidence for the transformation of the lithospheric structure of the Songliao Basin by three major tectonic systems. This paper uses 157 broadband magnetotelluric sounding data in the northern

Songliao Basin (Fig 1) to perform 3D magnetotelluric inversion giving the first electrical structure of crust and mantle in the area and explains the characteristics of the lithosphere under the superposition and transformation of the multi-phase structural system.

2 Research Method

2.1 Data collection and processing

The research area is located at an expanse of 120,000 square kilometers in northeastern China, including Heilongjiang Province, Jilin Province, and Liaoning Province (about 123°-127° east longitude and about 45°-49° north latitude). The basin is divided into five primary structural units according to the distribution and development characteristics of the fault depressions, namely; the central depression zone (Ⅰ), the southeast uplift zone (Ⅱ), the northeast uplift zone (III),the northern plunge zone (IV), and the west slope zone (V). Multiple secondary fault depressions and fault uplifts lie inside. This work uses a total of 157 broadband magnetotelluric sounding data points, of which 122 survey points were from the exploration work of Daqing Oilfield Research Institute from 1994 to 1999, and the remaining 35 survey points were from Jilin University from June 2017 to September 2018. MTU-5 magnetotelluric instruments produced by Phoenix Geophysics of Canada were used for field collection of magnetotelluric sounds and the effective frequency band was 320~0.0005 Hz. The poles were arranged according to the tensor measurement method. Each measuring point measures 5 components, 3 of them being magnetic field components while the other 2 are mutually orthogonal horizontal electric field components. The signal acquisition time was about 20 hours and the average point distance was 10 km.

During data processing SSMT2000 software was used to perform fast Fourier transform on the original time series, transforming the time domain signal into frequency domain data, thus obtaining high-quality impedance tensor information via processing techniques such as "Robust" estimation and power spectrum selection. Following a series of processing steps, the apparent resistivity and phase curves of all measuring points were acquired. The data quality of most measuring points was found to be good, and any sudden jump point in the frequency band was deleted before participating in the inversion.

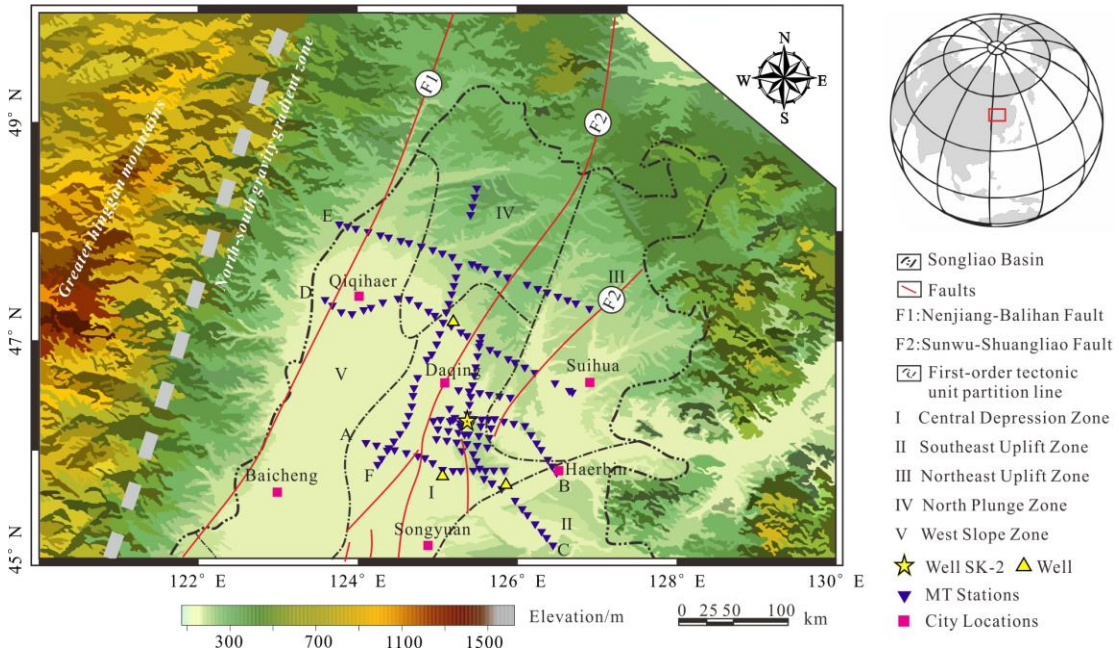

Figure 1. The location map of the magnetotelluric sounding line in the north of Songliao Basin

To verify the reliability of the data, three wells around the study area (see Fig1 for locations) (Linshen 2, Zhao 12 and Chaoshen 1 wells with depths of 3450 m, 3217 m, and 3052 m respectively) were utilized to calibrate the shallow electrical structure (Fig 2). The borehole resistivity logging results revealed that, except for a small range uplift of resistivity at a depth of 400 m, the other shallow electrical characteristics of 1200 m all showed low resistance of about a few Ω·m; the resistivity of 1200-3000m increased and was found to be directly proportional to the depth and grew rapidly to approximately 1000Ω·m. At around the same time, the geometric mean apparent resistivity of the nearest magnetotelluric sounding (MT) point around the well was selected for one-dimensional OCCAM inversion. The inversion results were found to be consistent with the trend of resistivity logging curves, showing "sudden jump-low-high resistance". The changing trend is sufficient evidence of the reliability of MT data.

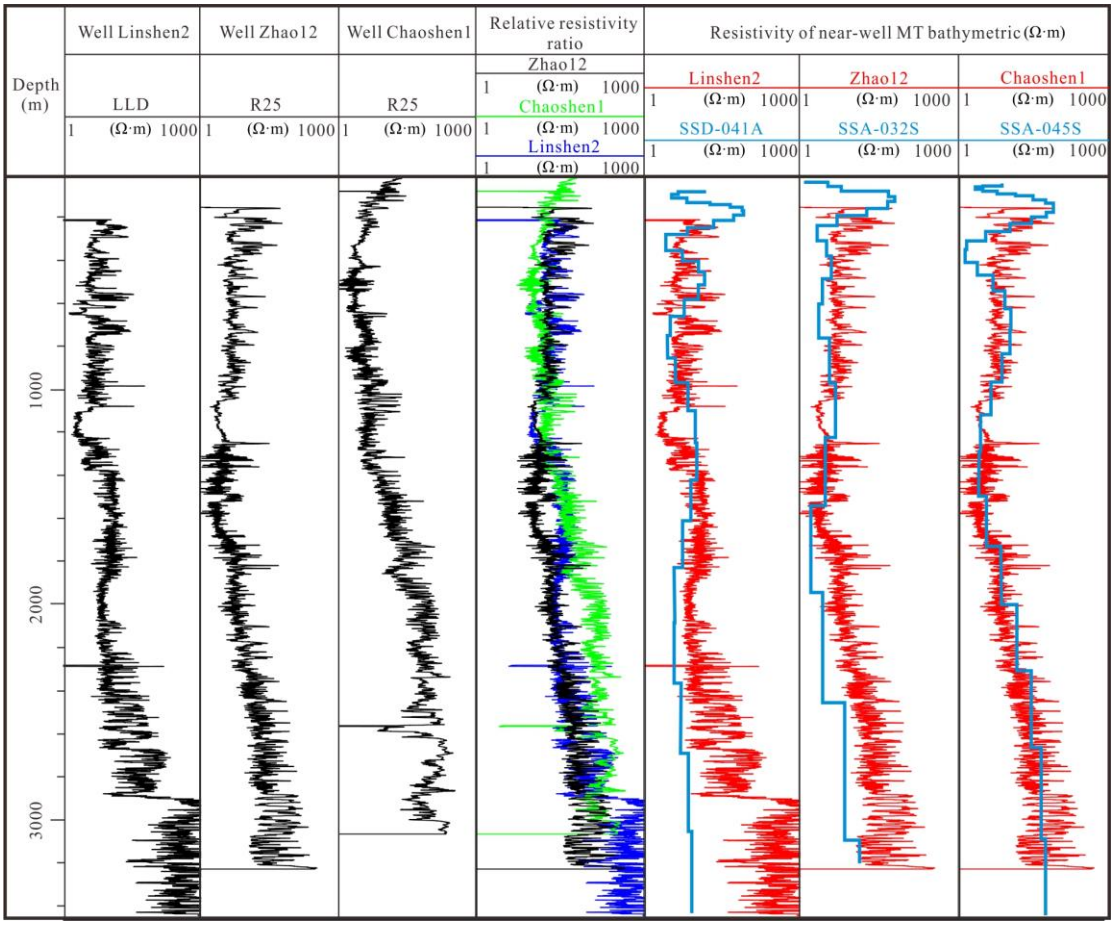

Figure 2. Comparison of the results of different borehole resistivity logs and near-hole magnetotelluric sounding

(In addition to the depth track, columns 1-3: Linshen2, Zhao12, Chaoshen1 resistivity logging curves; column 4: relative resistivity values; columns 5-7 show the joint mode of resistivity

logging and near-well earth electromagnetic sounding point 1D OCCAM inversion result comparison)

2.2 Dimensional analysis

To construct an electrical model that is an accurate reflection of the geological structure, it is imperative to perform data analysis before inversion. The phase tensor has an interesting characteristic of being less affected by the current distortion effect caused by the non-uniformity of the near-surface, and it has become a valuable parameter for analyzing the dimensionality of the region. Using 3D model studies, it has been illustrated that the direction of the principal axis of the phase tensor reflects the lateral changes in the conductivity structure of the underlying region (Caldwell et al., 2004). When the 2D deviation is 0 and the ellipse is approximately circular, the underground medium is considered to have a 1D characteristic whereas when the 2D deviation is 0 and the long and short axes of the ellipse are not equal, the underground medium is considered to have 2D characteristic; when the degree is non-0, it is a 3D medium, and 3D characteristic is proportional to the magnitude of 2D deviation. In general, when the absolute value of 2D deviation rises above 3°, it is expressed as a strong 3D characteristic (Caldwell et al., 2004).

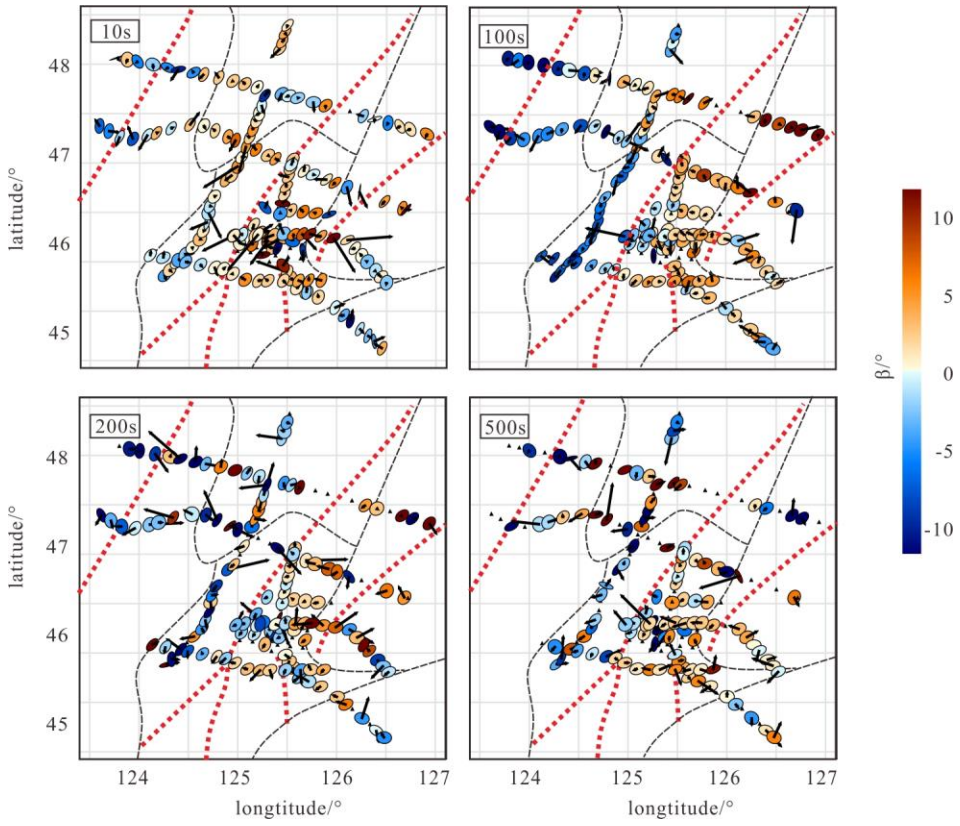

Figure 3. Horizontal distribution map of phase tensor of all frequency points in northern Songliao Basin

Fig 3 illustrates the sub-band phase tensor level distribution of all measurement points. The color of ellipse represents the value of the 2D deviation β, and ellipse azimuth of most measurement points in 4 periods (T) is N 20°E —N 40°E, particularly the azimuth angle of the main axis of the ellipse around the structural zone is basically along the structural direction. When T=10s, the 2D deviation of most measuring points was small and showed 1D and 2D characteristics. As the period increased, the 2D deviation value began showing an increasing trend, indicating that the part having depth has strong 3D characteristics. The direction of the major axis of the ellipse started becoming increasingly diverse, including NE, NW, and near EW directions, revealing the complex deep structure pattern of the area. The black arrow represents the real induction vector, its direction pointing to the high conductor (Parkinson, 1959), whereas the lateral unevenness is represented by the length of the arrow. From a macro perspective, the direction of the induction vector is chaotic, and the length is varying, especially in the middle of the central depression area. Perhaps, the good stratification in the shallow part of this area affected the orientation of the induction vector, thus pointing to the structural complexity of the Songliao Basin. Nevertheless, the direction of the induction vector mostly points to the location of the nearby fracture. The direction of the fracture is not unique but exists at least in two groups.

The color of the ellipse represents the two-dimensional deviation value, the black arrow represents the real induction vector, the thin black dotted line represents the division of the tectonic units within the basin (Fig. 1), the thick red dotted line represents the location of the known deep fault whereas the missing points represent the eliminated frequency

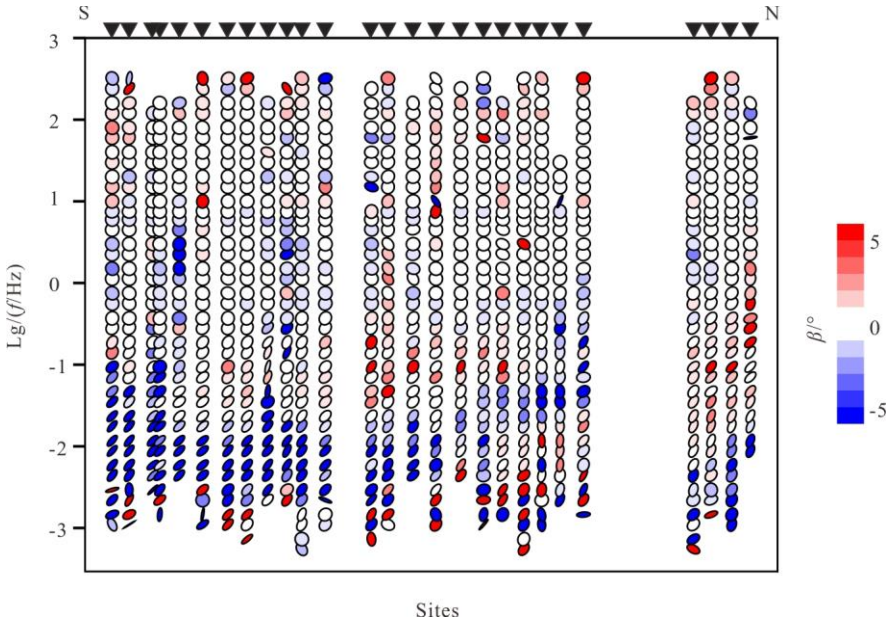

Figure 4. The results of phase tensor analysis of Line F in northern Songliao Basin

Fig. 4 represents the results of the phase tensor analysis of the Line F. Line F passes from south to north through the central depression zone and the northern plunge zone (Fig. 1). There is a larger period between 10 s and 1000 s on the southern side of Line F and 2D deviation degree and has a large ellipticity. The characteristics near the north gradually weakened, indicating that the deepest part of the central depression area has a strong 3D geological background which only weakens when it extends northward. Hence it is evident from the phase tensor analysis that the crust and mantle of the Songliao Basin have an obvious 3D characteristic, particularly in the central depression zone. Therefore, only 3D inversion can provide a more reliable electrical model.

2.3 Data inversion

Mod3DMT (Egbert & Kelbert, 2012) based on the nonlinear conjugate gradient (NLCG) algorithm was used to perform 3D inversion of the full impedance data of 157 measuring points. A uniform half-space of 100Ω·m is selected as the initial model, and the frequency lies in 1000-0.0001Hz range, grid division in X direction: grid length 5km, 70 grids, 5 grids on both sides expanded by a factor of 2.5; grid division in Y direction: grid length 5km, 90 grids, with 5 grids expanded on both sides by a factor of 2.5; grid division in the Z direction: first layer 50m, layer increment factor: 1.23, a total of 35 grids, and borders expanded by a factor of 2.5 5 grids. Adding 5% as noise, a total of 107 inversions were performed, and the RMS decreased from 44.18 to 2.95. Finally, a 3D geoelectric model of the lithosphere scale of the northern Songliao Basin was obtained.

2.4 Model validation

The distribution of total impedance RMS of 157 measuring points is illustrated in Fig.5. Except for s large fitting error of individual measuring points, the fitting error of most measuring points was concentrated between 1-3, which lies close in value to the overall fitting error. There is no over-fitting and under-fitting hence, proving the credibility of the 3D inversion model.

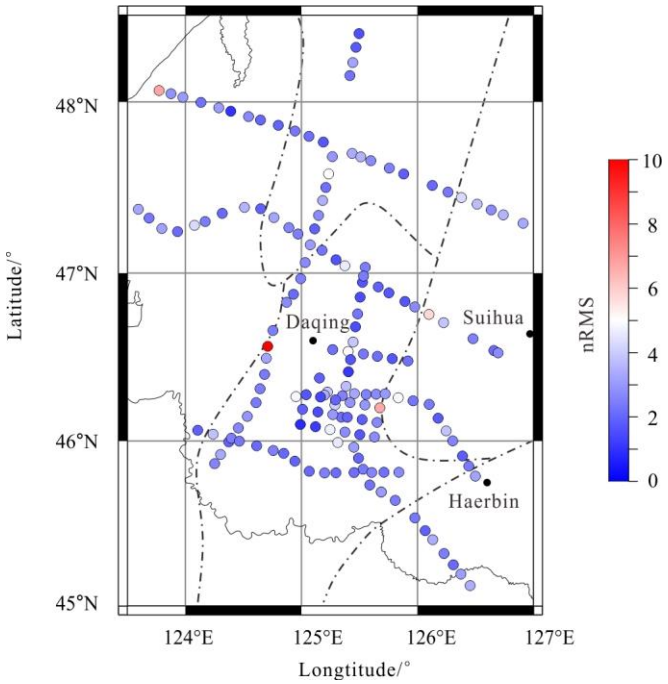

Figure 5. Fitting situation of all impedances of all sounding points of magnetotelluric sounding in northern Songliao Basin

The gray line indicates the provincial boundary; the dotted line indicates the division of the structural units within the basin (see Fig. 1), while the black circle indicates the location.

3 Electrical Structure Characteristics

To analyze the electrical characteristics of slices at different depths, the resistivity slices with depths of 5 km, 10 km, 15 km, 20 km, 30 km, and 50 km were selected corresponding respectively to the depth of shallow layer, the top surface of the basement (upper crust), upper and lower crust boundary, lower crust, Moho surface and upper mantle in the northern Songliao Basin. Electrical gradient bands and low-resistance anomalies are often the most common signs to identify the location of faults. While the interface of the resistance level conversion is often indicative of them being two different substances and that faults are prone to occur between them, on the other hand, faults or alteration zones provide a channel for magma to flow upwards, and there are generally broken and loose low-resistance media where the fault zone develops. Hence low-resistance anomalies appear in the electrical structure. After precisely combining the location of surface faults and electrical structural characteristics, the locations of the Binzhou fault zone, the Nehe-Suihua fault zone, Yi'an-Tongyu fault zone, Sunwu-Shuangliao fault zone, and Nenjiang-Balihan fault zone were determined (Fig.6).

Some anomalous complexities are exhibited by the 5 km underground slice. Only towards the north of the boundary between the northern plunge zone (IV) and the central depression zone (I), a connected high-conductivity anomaly C1 appears, with broken high-conductors in the NE-SE

and NW-SE directions. Preliminarily, it was inferred that C1 is the intersection of NE and NW trending faults/fault depressions in the shallow part. The high resistance anomalies in this depth range reflect the placement of the volcanic rock aggregates. The horizontal slice having a depth of 10 km, has low-resistance anomalies that are found to be distributed in the western slope zone (V), the northern plunge area (IV), the central depression zone (I), and the northeast uplift zone (III), with a resistivity lower than 15Ω· M, the high-conductivity anomaly at this depth initially spreads in the NW and NE directions compared to the electrical structure of shallower slices. At depths of 15 km, 20 km, and 30 km, the range of high-conductivity anomalies is comparatively wide, and there were band-shaped high-conductivity anomalies in NW, NE, and EW direction with a resistivity value of about 10Ω· m. The multitropism of the depth anomaly suggests that the northern Songliao Basin has experienced the superposition of many tectonic systems, rather than a single structural realm. In the study of the Man-Sui section, a consensus was reached on the existence of low-velocity, low-density, and high-conductivity layers at a depth of 15-25 km, and it is believed that the plastic middle-lower crust is fluid rich. So, the high conductivity anomalies in the NW and NE directions are most likely a fluid-rich fracture system. The contours of low- and medium-resistance anomalies below 30Ω·m at a depth of 50 km continue the 30-km high-conductivity anomaly. It is worth noting that a large region of near-south high conductivity anomaly lies at the junction of the central depression zone and the northern subduction zone, having a longitudinal expanse of several tens of kilometers, which is presumably a manifestation of substance upheaval in the deep asthenosphere in this area.

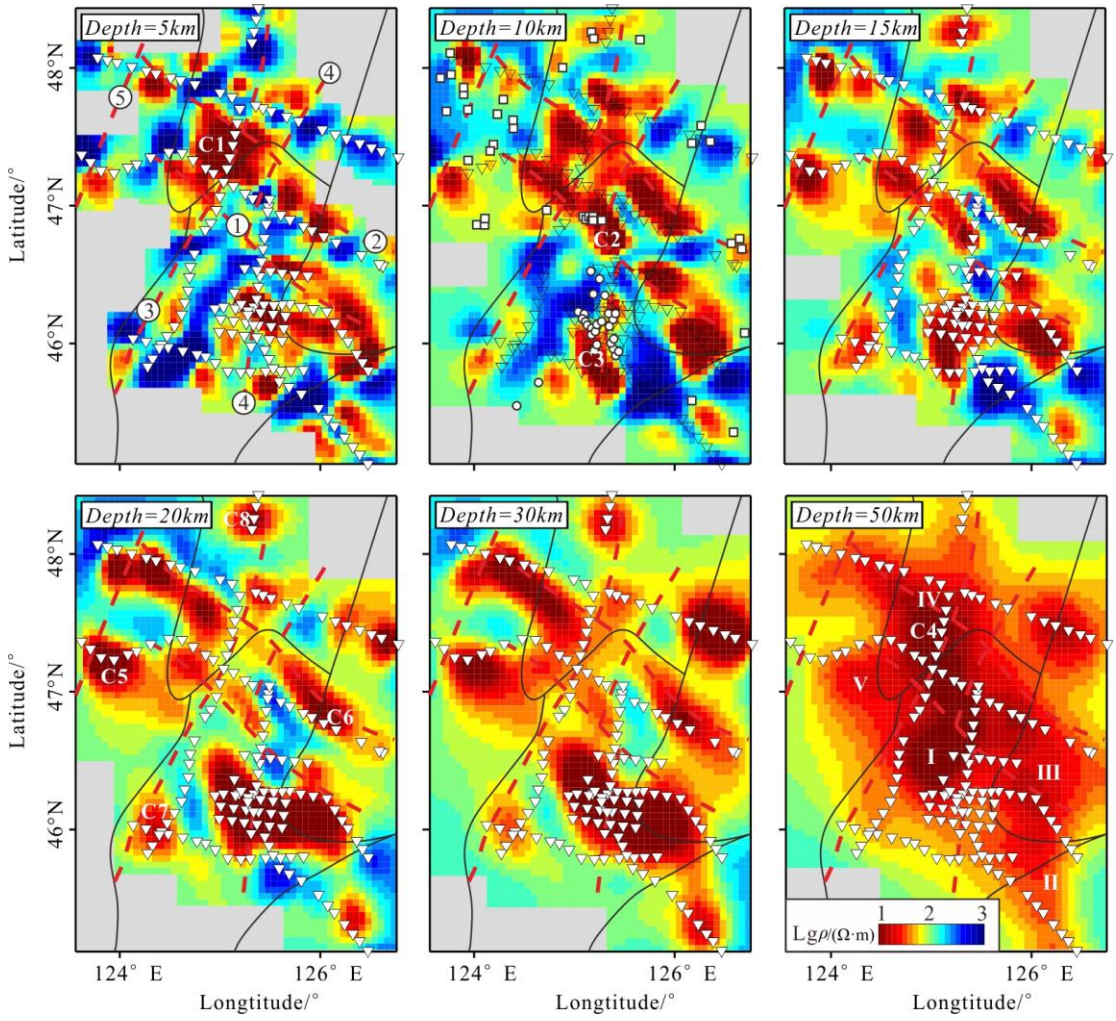

Figure 6. Horizontal slice of the 3D electrical structure in the northern Songliao Basin.

The white inverted triangle is the location of the measuring point; the white square is the focal location of the earthquake in the area (average focal depth at C2 is 8.625km) (data from China Seismic Network); the white circle is the location of the well that encountered CO_2 (according to Zhang et al., 2009); the black dotted line demarcates the boundary of the structural unit; the black dense line is fault zone ①Binzhou fault zone ②Nehe-Suihua fault zone ③Yi'an-Tongyu fault zone ④Sunwu-Shuangliao fault zone ⑤Nenjiang-Balihan fault zone

4 Discussion

4.1 Upper crustal material composition

Underneath the Cenozoic sedimentary caprock in the Songliao Basin, there is a relatively complete Cretaceous stratum. The early Cretaceous layer formed fault depressions after experiencing the evolutionary history of the fault depression period, including Yingcheng, Shahezi, and Huoshiling formations. The seismic cross-section through the

Songliao Basin shows that the burial depth of the faulted layer is 2~5 km, and it has obvious characteristics of being deep in the middle and shallow on both sides. During this period, the asthenosphere upwelled due to the subduction of the Pacific plate, the lithosphere squeezed and stretched, the crust straightened and cracked, several crust faults appeared, and a fairly good number of magma intrusions and eruptions developed along the faults. Brittle deformation occurred and the land of the upper crust sank, forming a series of faulted basins distributed in the NNE direction (Wang et al., 2016).

The 5 km electrical slice showed an obvious crisscrossing high-conductivity anomaly C1, seemingly caused by the superposition of two-way faults/fault depressions, which exhibit high-conductivity features that cross each other. Existing data show that the NW and NE-trending faults in the basin form an orthogonal grid-like extensional fault system, dividing the Songliao Basin into east-west zones and the north-south block structure, which is consistent with the electrical structure investigated and mentioned in this work. Due to the frequent occurrence of volcanic magmatism in the Songliao Basin since the Mesozoic (Wu et al., 2005; Zhang et al., 2010), volcanic rocks are quite widespread. Drilling, seismic, gravity, and magnetic data show that deep volcanic rocks in the Songliao Basin are widely distributed in the Jurassic Huoshiling Formation and Early Cretaceous Yingcheng Formation (Wei et al., 2019). The distribution map of aggregates of volcanic rock predicted by regional earthquakes (Zhang et al., 2010), is found to be consistent with the NE-direction high-resistance anomaly position, so the high-resistance anomaly within a depth of 5 km is inferred as volcanic rock. In the 10 km depth slice, there are two NW-direction high conductivity anomalies, C2 and C3, respectively corresponding to the seismically dense area and the location of the well, where CO_2 is drilled in the region (Fig. 6) hence proving that C2 and C3 are avenues for the occurrence of earthquakes and the migration of CO_2 for the fracture system inside the crust at this depth.

Viewed together, the geological background and the electrical structure of 5km and 10km slices, it can be estimated that locally distributed volcanic rock bodies, NE, and NW-oriented faults/fault depressions together constitute the key structural elements of the upper crust of the Songliao Basin.

4.2 Lithosphere thinning in Songliao Basin

A large volume of evidence suggests a thinning of the lithosphere in the Songliao Basin. Surface wave imaging studies showed that the lower part of the Songliao Basin is a thin lithospheric caprock, with a thickness much less than the average thickness of the continental lithosphere (Ren et al., 2002; Meng., 2003; Guo et al., 2014). The images released by the broadband seismic stations in Northeast China show that the average depth of the Lithospheric Asthenosphere Boundary (LAB) in the Songliao Basin is about

80 km. The shallowest part lies below the center of the basin, and geological cross-section data showed that the thickness of the lithosphere near Anda in the Songliao Basin is only 60 km (Cheng and Wu, 1994). The thinning of the lithosphere was generally believed to be related to the extension of the Mesozoic lithosphere, and its direct stress is derived from the undercutting of magma. Studies have found that the uppermost surface of the asthenosphere below the basin presents an upwardly convex arc (Guo et al., 2014). The largest part of the depression of rift valley in the Songliao Basin corresponds to the upheaving region of the asthenosphere (Han et al., 2018), but earlier researches have not pointed out the extreme point of lithospheric thinning, that is, the center of the upwelling of the asthenosphere area. In this investigation, which is based on a 50 km mantle-scale horizontal slice, it has been found that there is a sizeable region of high conductivity anomaly C4 lying under the Lindian fault depression located at the junction of the central depression zone and the northern plunge zone, and covering an area of tens of kilometers in the SN direction in the longitudinal slice. It has an uplifted shape with a top interface of 45 km, which can be inferred to be the center of the asthenosphere upwelling. It authenticates the existence of a relatively thin lithosphere in the Songliao Basin as well as the continuous erosion of the bottom interface of the lithosphere due to the under-intrusion of the asthenosphere (Kuritani et al., 2011; Liu et al., 2016), thus forming an uplift of the asthenosphere and gradually transforming the lithosphere into new-born rocks with a high conductivity characteristics ring. It is worth mentioning that the center of the upwelling of the asthenosphere is located below the Lindian fault depression, and the shallowest part is 45 km deep.

4.3 The remaining traces of the three major structural systems in the Songliao Basin

The evolution of the Songliao Basin has undergone superimposed transformation of three major structural domains of the Paleo-Asian Ocean, Mongolia-Okhotsk, and Paleo-Pacific (Wang et al., 2017; Liu et al., 2017; Wu et al., 2011; Xu et al., 2013). Despite the superposition and transformation of the later structural domains, the remnants of the pre-existing structural system can still be observed. There was a deep seismic reflection profile in the same direction as SN in the vicinity of Line F, which recorded the tectonic events of south-to-north subduction during the closure of the Paleo-Asian Ocean and the subduction residue of a block during the closure of the eastern Mongolian-Okhotic Ocean (M3 and M4 in Fig. 7). The east-west sloping lower crust reflections and mantle reflections (M1 and M2 in Fig. 7), existing in the seismic profile on the same location as line D are considered to be the result of the overlap of each other, subduction compression and strong extension that occurred later between Mongolia-Okhotsk tectonic domain and the paleo-Pacific tectonic domain in the deep part of the Songliao Basin (Fu et al., 2019).

Early subduction residues and bidirectional convergence splice marks revealed by deep seismic reflections verified that the Songliao Basin was once in a compression environment under the action of the tectonic system. Due to the continuous impact of external stress, the crust-mantle was vulnerable to damage, resulting in a structurally weak zone or a patchy unstable zone. The Mongolia-Okhotsk tectonic system and the Paleo-Pacific tectonic system are related with respect to time and space, and the two intersect during the transformation of the Jurassic and Cretaceous (Fu et al., 2019), through the combination of volcanic rocks. The distribution characteristics in time and space found that the spatial scope of the influence of the Pacific Rim tectonic system in the East Asian continent lies mainly in the Songliao Basin and its east whereas the spatial scope of the Mongolia-Okhotsk structure system is primarily lying in the west of the Songliao Basin and the edge of North China (Xu et al., 2013). Hence, the Songliao Basin belongs to the joint action area of the two tectonic systems. The closure of the Mongolia-Okhotsk Ocean and the dehydration of the Pacific slab trapped in the mantle transition zone, set off asthenospheric upwelling, filling the weak structural zone or the unsteady assembly zone that had been left behind, leading to its activation and becoming a partial melt, thus providing a channel for the upward migration. Therefore, the structural system should have a corresponding performance on the geoelectric structure. The fact that the remains of the tectonic system correspond to the magma channel is not accidental. The joint seismic section (Li et al., 2014) passing through the northern margin of North China and the southern part of the CAOB also found, low-velocity gradient, and channel-like in lower crustal. It was speculated that it may have been an active continental margin where the Paleo-Asian Ocean subducted and died southward, and evolved into a channel for magma intrusion in an extensional environment following the collision.

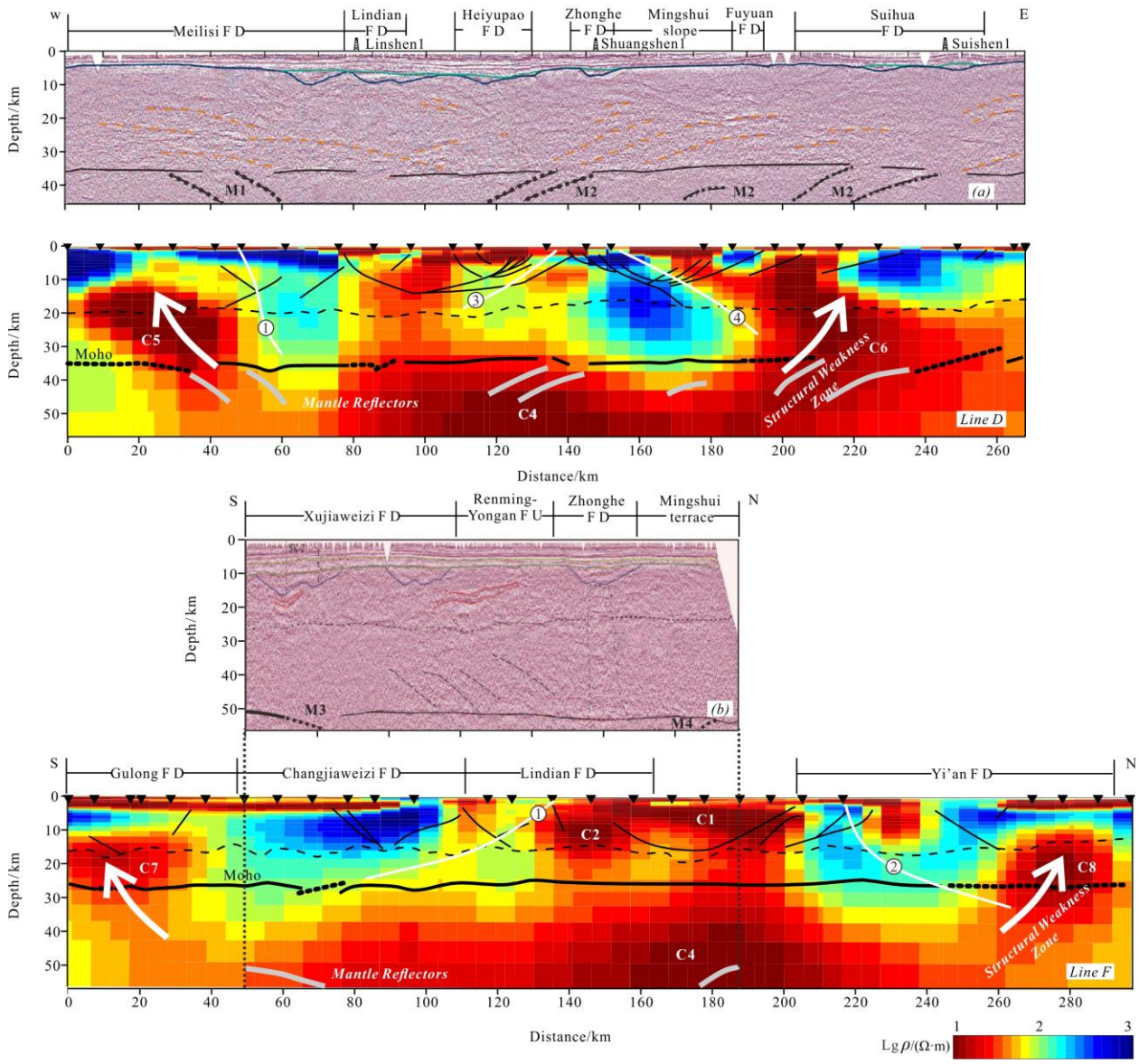

Figure 7. Comparison and interpretation of the deep reflection seismic profile (Fu et al., 2019) and 3D electrical structure longitudinal slices in the northern Songliao Basin. (a) coincides with the position of Line D section, (b) is in the same direction as Line F, and is about 40km apart.

FD stands for fault depression; FU stands for fault uplift; M stands for mantle reflection during the earthquake, M1 designates residual traces of north-south subduction tectonic events during the closure of the Paleo-Asian Ocean, M2 designates residual subduction of a block during the closure of the eastern Mongolia-Ekhotsk Ocean, M3 designates subduction traces under the action of the Mongolian-Okhotsk Ocean, M4 designates subduction traces under the action of the ancient Pacific Ocean (Fu et al., 2019); the thin black line is the tectonic line in the seismic crust; the thick line is the depth of the Moho surface (according to Sun, 2019); the dotted line in the middle and lower crustal interface for seismic identification (according to Wang, 2015); thin

379 white lines indicate the fault zone ①Binzhou fault zone ②Nehe-Suihua fault zone ③Yi'an-
380 Tongyu fault zone ④Sunwu - Shuangliao fault zone ⑤Nenjiang- Balihan fault zone.

This investigation selected the longitudinal slices in the same direction and close to the seismic profiles for analysis, which include the Line D in the NW direction and the Line F in the near SN direction. The depth of the Moho is about 30 km (Wang et al., 2016), and the ups and downs of the Moho are drawn according to the Songshen deep seismic reflection profiles (Yang et al., 2004). In the lower crust, there are low-resistance anomalies C5, C6, C7, and C8 that cross the Moho, and the Moho at the bottom is missing and overlap to varying degrees. The electrical results show that the high-conductivity layer in the crust originates from the upper mantle, so the absence and overlap of the Moho may be caused by the upwelling of asthenospheric materials to the interception of the lower crust by the brittle-ductile shear zone. It is worth noting that a large number of high-conductivity layers in the mantle are filled below 30 km, with a resistivity value of more than ten Ω·m, and a slight uplift in the middle which is quite prominent on both sides, and are connected with high-conductivity anomalies under the crust of the Gulong and Yian fault depressions, Meilis and Suihua fault depressions respectively. Although the traces of subduction residues cannot be distinguished in the electrical section in terms of relative position and burial depth, the upwelling high conductivity anomalies C5, C6, C7, and C8 on both sides of the Line D and Line F may be the paleo-shear zones formed during the microcontinental assemblage when the Paleo-Asian Ocean was closed. (Yang et al., 2001). The combination of the closure of the Mongolian-Okhotsk Ocean and the subduction of the Paleo-Pacific Ocean reactivated the paleo-shear zones. Due to the dehydration of the Pacific plate lying in the mantle transition zone (Kimura et al., 2018; Kuritani., 2011, 2019), the paleo-shear zones were filled with upwelling asthenosphere material, thus showing the high conductivity, characteristic of the connection with the upper mantle.

Therefore, we propose a schematic cartoon of the geoelectrical model presented above (Fig. 8). During the tectonic regime of the Paleo-Asian Ocean, the Paleo-Asian Ocean was continuously consumed, the Songnen block, where the Songliao Basin is located, was closing to the adjacent microcontinental blocks one after another. The intense squeezing action resulted in several palaeo-shear zones in the lower part of the Songliao Basin (Fig. 8a). The period when the Mongolian-Okhotsk and the paleo-Pacific tectonic systems worked together, the Mongolia-Okhotsk Ocean and the Paleo-Pacific Ocean respectively acted on the northwest and east sides of Songliao Basin. The two-way converging ocean slabs reactivated the paleo-shear zones. The later dehydration of the Pacific slab stimulated the asthenospheric material to rise along these weak zones allowing the paleo-shear zones to be "marked" in the geoelectrical model (Fig. 8b).

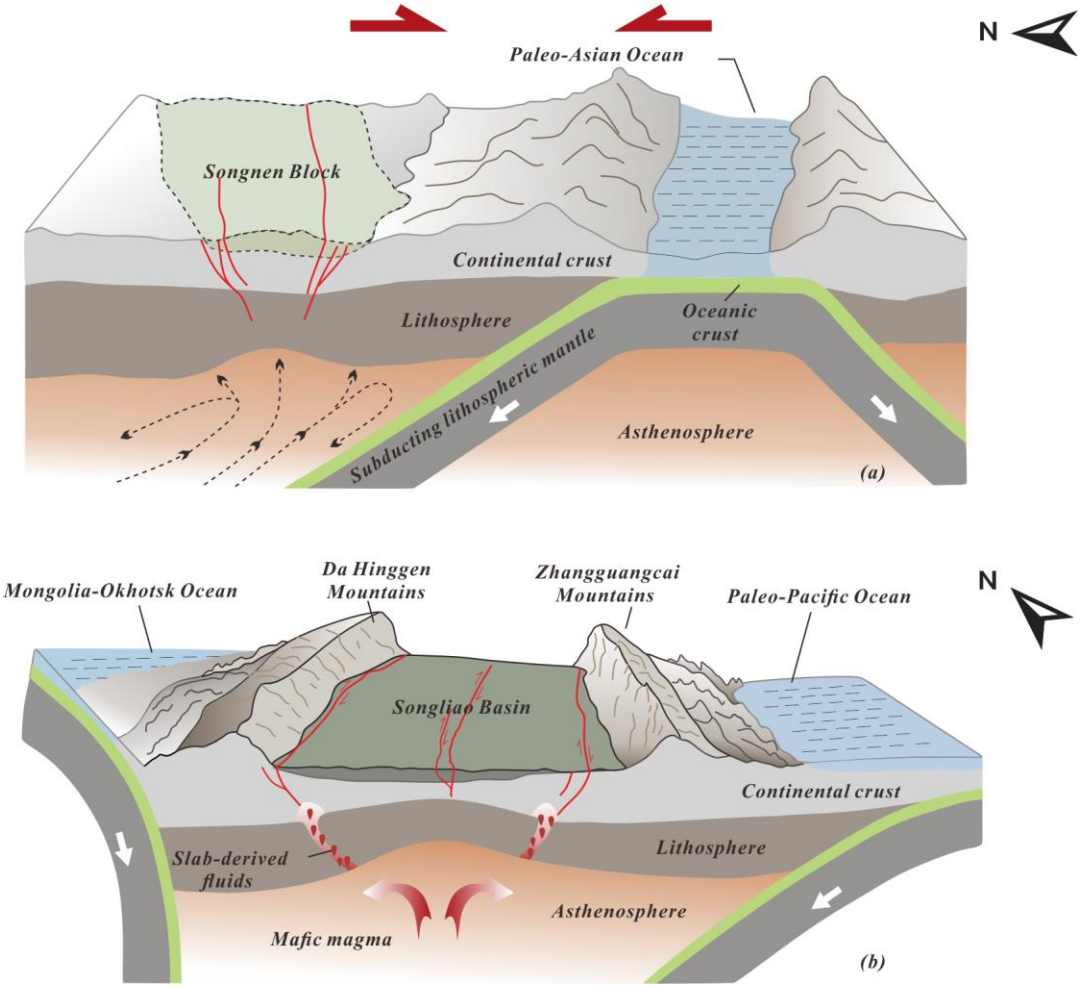

Figure 8. Schematic cartoon of the geoelectrical model. (a) represents the period when the Paleo-Asian ocean tectonic system was in effect (according to Li, et al., 2016, 2017). (b) represents the period when the Mongolian-Okhotsk and the paleo-Pacific tectonic systems worked together (according to Cheng, et al., 2018).

5 Conclusions

In this work, the full-impedance magnetotelluric 3D inversion of the magnetotelluric sounding profile is carried out in the northern Songliao Basin, and a 3D electrical structure model is established. Based on the characteristics of the electrical structure of the slices electrical structure, we arrive at the following conclusion:

1) Based on the distribution and electrical structural characteristics of volcanic rocks predicted by earthquakes, it has been found that the volcanic rock clump is consistent with the location of NE-trending high-resistance anomalies, while the scattered low-resistances distributed in the NE and NW directions correspond to the location of faults

/fault depressions. It has been inferred that the upper crust of the northern Songliao Basin is composed of volcanic rocks and faults /fault depressions;

2) Mesozoic underplating set off the extension of the lithosphere in the Songliao Basin, resulting in an uplifted shape on the top of the asthenosphere in the Songliao Basin. The most prominent part of the uplift is located at the junction of the central depression zone and the northern submerged area (Below the Lindian Fault Depression). The buried depth is 45 km, which is the center of the upwelling of the asthenosphere hot material;

3) It has been found that there is a set of symmetrically distributed high conductivity regions under the crust of the Gulong and Yian fault depressions, Meilis and Suihua fault depressions respectively in the Songliao Basin. This peculiarity can be attributed to the weak tectonic zone produced by the “Paleo-shear” effect during the closure of the Paleo-Asian Ocean. Afterwards they were reactivated by the continuous transformation of the Mongolia-Okhotsk tectonic domain and the Paleo-Pacific tectonic system in the later period.

Acknowledgments

This study is supported by the National Key R&D Program of China (2017YFC0601305), the National Natural Science Foundation of China (41504076), the China Geological Survey Project (DD20160207), the Jilin Scientific and Technological Development Program (20180101093JC). Several figures are plotted using the MtPy software (Krieger and Peacock, 2014; Kirkby et al., 2019). The data archiving is underway in https://www.pangaea.de/, and the copy data has been uploaded in supporting information (SI).

References

Aizawa, K., Koyamal, T., Hase, H., Uyeshimal, M., Kanda, W., Utsugit, M., et al. (2014). Three-dimensional resistivity structure and magma plumbing system of the Kirishima Volcanoes as inferred from broadband magnetotelluric data. *Journal of Geophysical Research*, 119, 198-215. http://doi.org/10.1002/2013JB010682

Caldwell, T. G., Bibby, H. M., Brown, C. (2004). The magnetotelluric phase tensor, *Geophysical Journal International*, 158(2), 457-469. http://doi.org/10.1111/j.1365-246x.2004.02281.x

Cheng, Y., Wang, S., Li, Y., Ao, C., Li, Y., Li, J., et al. (2018). Late Cretaceous-Cenozoic thermochronology in the southern Songliao Basin, NE China: New insightsfrom apatite and zircon fission track analysis. *Journal of Asian Earth Sciences*, 16095-106. https://doi.org/10.1016/j.jseaes.2018.04.015

Cheng, Z S., Wu, X Y., A study of lithosphere electronic structure in Manzhouli-Suifenhe GGT[A]. In: Jin X, ed.A study of geophysical field and deep tectonic characteristics in Manzhouli-Suifenhe GGT[C]. Beijing: Earthquake Publishing House,1994.45-58.

Egbert, G., Kelbert, A. (2012). Computational recipes for electromagnetic inverse problems. *Geophysical Journal International*, 189, 251-267. https://doi.org/10.1111/j.1365-246X.2011.05347.x

Fu, W., Hou, H., Gao, R., Liu, C., Yang, J., Guo, R. (2019). Fine structure of the lithosphere beneath the Well SK-2 and its adjacent: Revealed by deep seismic reflection profile. *Chinese Journal of Geophysics*. 62(4):1349-1361, http://doi.org/10.6038/cjg2019M0370

Guo, Z., Cao, Y., Wang, X., Chen, Y., Ning, J., He, W., et al. (2014). Crust and upper mantle structures beneath Northeast China from receiver function studies. *Eathquake Science*, 27, 265-275, https://doi.org/10.1007/s11589-014-0076-x

Han, J., Guo, Z., Liu, W., Hou, H., Liu, G., Han, S., et al. (2018). Deep dynamic process of lithosphere thinning in Songliao basin. *Chinese Journal of Geophysics*. 61(6):2265-2279, http://doi.org/10.6038/cjg2018L0155

He, C., Santosh, M. (2016). Seismic tomographic evidence for upwelling mantle plume in NE China. *Physics of the Earth and Planetary Interiors*, 254: 37-45, https://doi.org/10.1016/j.pepi.2016.05.020

Heise, W., Caldwell, T. G., Bibby, H. M., Bannister, S. C. (2008). Three-dimensional modelling of magnetotelluric data from the Rotokawa geothermal field, Taupo Volcanic Zone, New Zealand. *Geophysical Journal International*, 173, 740-750, https://doi.org/10.1111/j.1365-246X.2008.03737.x

Jian, P., Liu, D., Kröner, A., Windley, B. F., Shi, Y., Zhang, F., et al. (2008). Time scale of an early to mid-Paleozoic orogenic cycle of the long-lived Central Asian Orogenic Belt, Inner Mongolia of China: Implications for continental growth. *Lithos*, 101(3-4):233-259. https://doi.org/10.1016/j.lithos.2007.07.005

Kimura, J. I., Sakuyama, T., Miyazaki, T., Vaglarov, B. S., Fukao, Y., Stern, R. J. (2018). Plume-stagnant slab-lithosphere interactions: Origin of the late Cenozoic intra-plate basalts on the East Eurasia margin. *Lithos* 300-301, 227-249. https://doi.org/10.1016/j.lithos.2017.12.003

Kirkby, A. L., Zhang, F., Peacock, J., Hassan, R., Duan, J. (2019). The MTPy software package for magnetotelluric data analysis and visualisation. *Journal of Open Source Software*, 4(37), 1358. https://doi.org/10.21105/joss.01358

Krieger, L., Peacock, J. (2014). MTpy: A Python toolbox for magnetotellurics. *Computers and Geosciences*, 72, p167-175. https://doi.org/10.1016/j.cageo.2014.07.013

Kuritani, T., Ohtani, E., Kimura, J. I. (2011). Intensive hydration of the mantle transition zone beneath China caused by ancient slab stagnation. *Nature Geoscience*, 4, 713–716. https://doi.org/10.1038/ngeo1250

Kuritani, T., Xia, Q.-K., Kimura, J. I., Liu, J., Shimizu, K., Ushikubo, T., et al. (2019). Buoyant hydrous mantle plume from the mantle transition zone. *Scientific Reports*, 9(6549). https://doi.org/10.1038/s41598-019-43103-y

Li, S., Weng, A., Li, J., Shan, X., Han, J., Tang, Y., et al. (2020). Deep origin of Cenozoic volcanoes in Northeast China revealed by 3-D electrical structure. *Science China Earth Sciences*, 63:533-547. https://doi. org/10.1007/s11430-018-9537-2

Li, W., Gao, R., Randy, K., Li, Q., Hou, H., Li, Y., et al. (2014). Crustal structure of the northern margin of north China craton from Huailai to Sonid Youqi profile. *Chinese Journal of Geophysics*, 57(2):472-483. https://doi.org/10.6038/cjg20140213.

Li, Y., Brouwer, F. M., Xiao, W., Zheng, J. (2016). Late Devonian to early Carboniferous arc-related magmatismin the Baolidao arc Inner Mongolia, China: Significance for southward accretion of the eastern Central Asian orogenic belt. *Geological Society of America Buletin*,129(5-6),677-697. https://doi.org/10.1130/B31511.1

Li, Y., Brouwer, F. M., Xiao, W., Zheng, J. (2017). A Paleozoic fore-arc complex in the eastern Central Asian Orogenic Belt: Petrology, geochemistry and zircon U-Pb-Hf isotopic composition of paragneisses from the Xilingol Complex in Inner Mongolia, China. *Gondwana Research*, 47, 323–341. https://doi.org/10.1016/j.gr.2017.02.004

Liu, Y., Li, W., Feng, Z., Wen, Q., Neubauer, F., Liang, C. (2017). A review of the paleozoic tectonics in the eastern part of central asian orogenic belt. *Gondwana Research*, 43,123-148. https://doi.org/10.1016/j.gr.2016.03.013

Meng, Q. (2003). What drove late Mesozoic extension of the northern China-Mongolia tract? *Tectonophysics*, 369(3-4), 155–174. https://doi.org/10.1016/S0040-1951(03)00195-1

Miao, L., Fan, W., Liu, D., Zhang, F., Shi, Y., Guo, F. (2008). Geochronology and geochemistry of the Hegenshan ophiolitic complex: Implications for late-stage tectonic evolution ofthe Inner Mongolia-Daxinganling Orogenic Belt, China. *Journal of Asian Earth Sciences*, 32（5-6）：348-370. https://doi.org/10.1016/j.jseaes.2007.11.005

Parkinson, W. D. (1959). Directions of Rapid Geomagnetic Fluctuations. *Geophysical Journal International*, 2(1), 1–14. https://doi.org/10.1111/j.1365246x.1959.tb05776.x

Peacock, J. R., Mangan, M. T., McPhee, D. K., Ponce, D. A. (2015). Imaging the magmatic system of Mono Basin, California, with Magnetotellurics in three dimensions. *Journal of Geophysical Research*, 120, 7273-7289. https://doi.org/10.1002/2015JB012071

Ren, J., Tamaki, K., Li, S., Zhang, J. (2002). Late Mesozoic and Cenozoic rifting and its dynamic setting in eastern China and adjacent areas. *Tectonophysics*, 344(3-4), 175–205. https://doi.org/10.1016/S0040-1951(01)00271-2

Shan, X., Qin, S., Zhang, Y., Yang, B., Wang, M. (2009). Seismic evidence and geological significance of thrust-extension structure in upper basement of north Songliao Basin. *Chinese Journal of Geophysics*, 52(8): 2044~2049, https://doi.org/10.3969/j.issn.0001-5733.2009.08.012

Siripunvaraporn, W., Egbert, G., Lenbury, Y., Uyeshimaet, M. (2005). Three-dimensional magnetotelluric inversion: Data-space method. *Physics of the Earth and Planetary Interiors*, 150, 3-14. https://doi.org/10.1016/j.pepi.2004.08.023

Sun, C. (2019). The research of the basement tectonic characteristics of Songliao basin based on geophysical methods. Jilin University, MA thesis.

Tao, K., Niu, F., Ning, J., Chen, Y., Grand, S., Kawakatsu, H., et al. (2014). Crustal structure beneath NE China imaged by NECESSArray receiver function data. *Earth and Planetary Science Letters*, 398, 48–57. https://doi.org/10.1016/j.epsl.2014.04.043

Wang, J., Li, C. (2018). Curie point depths in northeast china and their geothermal implications for the songliao basin. *Journal of Asian Earth Sciences*, 163, 177-193. https://doi.org/10.1016/j.jseaes.2018.05.026

Wang, M. (2010). Thermal History Reconstruction of Upper Paleozoic in the North of Songliao Basin. Jilin University, PhD dissertation.

Wang, P., Xie, X., Frank, M., Ren, Y., Zhu, D., Sun, X. (2007). The cretaceous Songliao basin: Volcanogenic succession, sedimentary sequence and tectonic evolution, NE China. *Acta Geologica Sinica-English Edition*, 81(6): 1002-1011. https://doi.org/10.1111/j.1755-6724.2007.tb01022.x

Wang, P., Mattern, F., Didenko, N, A., Zhu, D., Singer, B., Sun, X. (2016). Tectonics and cycle system of the Cretaceous Songliao Basin: An inverted active continental margin basin. *Earth-Science Reviews*, 159, 82–102. https://doi.org/10.1016/j.earscirev.2016.05.004

Wang, T., Tong, Y., Zhang, L., Li, S., Huang, H., Zhang, J., et al. (2017). Phanerozoic granitoids in the middle and eastern parts of Central Asia and their tectonic significance, *Journal of Asian Earth Sciences*, 145, 368-392. http://doi.org/10.1016/j.jseaes.2017.06.029

562 Wang, Y. (2006). The onset of the Tan-Lu (Tancheng-Lujiang) fault movement in eastern
563 China: constraints from zircon (SH RIMP) and $^{40}Ar/^{39}$ Ar dating. *Terra Nova*, 18(6): 423-
564 431. https://doi.org/10.1111/j.1365-3121.2006.00708.x

565 Wannamaker, P. E., Hasterok, D. P., Johnston, J. M., Stodt, J. A., Hall, D. B., Sodergren, T. L.,
566 et al. (2008). Lithospheric dismemberment and magmatic processes of the Great Basin–
567 Colorado Plateau transition, Utah, implied from magnetotellurics. *Geochemistry, Geophysics, Geosystems*, 9(5), Q05019. http://doi.org/10.1029/2007gc001886

569 Wei, W., Unsworth, M., Johns, A., Booker, J., Tan, H., Nelson, D., et al., (2001). Detection of
570 widespread fluids in the Tibetan crust by magnetotelluric studies. *Science*, 292, 716–719.
571 http://doi.org/10.1126/science.1010580

572 Wei, W., Hammond, J. O. S., Zhao, D., Xu, J., Liu, Q., Gu, Y. (2019). Seismic evidence for a
573 mantle transition zone origin of the Wudalianchi and Halaha volcanoes in northeast China.
574 *Geochemistry, Geophysics, Geosystems*, 20, 398-416.
575 https://doi.org/10.1029/2018GC007663

576 Wu, F., Lin, J., Wilde, S. A., Zhang, X., Yang, J. (2005). Nature and significance of the Early
577 Cretaceous giant igneous event in eastern China. *Earth and Planetary Science Letters*,
578 233(1-2), 103–119. https://doi.org/10.1016/j.epsl.2005.02.019

579 Wu, F., Sun, D., Ge, W., Zhang, Y., Grant, M. L., Wilde, S. A., et al. (2011). Geochronology of
580 the Phanerozoic granitoids in northeastern China. *Journal of Asian Earth Sciences*, 41, 1–
581 30. https://doi.org/10.1016/j.jseaes.2010.11.014

582 Xiao, W., Windley, B. F., Hao, J., & Zhai, M. (2003). Accretion leading to collision and the
583 Permian Solonker suture, Inner Mongolia, China: Termination of the central Asian orogenic
584 belt. *Tectonics*, 22(6), 1069-1089. https://doi.org/10.1029/2002tc001484

585 Xu, W., Ji, W., Pei, F., Meng, E., Yu, Y., Yang D B., et al. (2009). Triassic volcanism in
586 eastern Heilongjiang and Jilin provinces, NE China: Chronology, geochemistry, and
587 tectonic implications. *Journal of Asian Earth Sciences*, 34(3), 392-402.
588 https://doi.org/10.1016/j.jseaes.2008.07.001

589 Xu, W., Pei, F., Wang, F., Meng, E., Ji, W., Yang, D., et al. (2013). Spatialtemporal
590 relationships of Mesozoic volcanic rocks in NE China: Constraints on tectonic overprinting
591 and transformations between multiple tectonic regimes. *Journal of Asian Earth Sciences*,
592 74, 167–193. https://doi.org/10.1016/j.jseaes.2013.04.003

593 Xu, W., Wang, F., Pei, F., Meng, E., Tang, J., Xu, M., et al. (2013). Mesozoic tectonic regimes
594 and regional ore-formingbackground in NE China: Constraints from spatial and temporal
595 variations of Mesozoic volcanic rock associations. *Acta Petrologica Sinica*, 29(2), 339-
596 353.

Yang, B., Tang, J., Li, Q., Wang, J., Faisal, S. A., Li, R., et al. (2004). Crustal reflection structure in the uplifting zone of Songliao Basin and disconnecting Moho interface. *Science in China Series D: Earth Science*, 47(6), 514–521. https://doi.org/10.1360/02yd0122

Zeng, S., Hu, X., Li, J., Xu, S., Fang, H., Cai, J. (2015). Detection of the deep crustal structure of the Qiangtang terrane using magnetotelluric imaging. *Tectonophysics*, 661, 180-189. https://doi.org/10.1016/j.tecto.2015.08.038

Zhang, H., Huang, Q., Zhao, G., Guo, Z., Chen, Y. (2016). Three-dimensional conductivity model of crust and uppermost mantle at the northern Trans North China Orogen: evidence for a mantle source of Datong volcanoes. *Earth and Planetary Science Letters*, 453, 182-192. https://dx.doi.org/10.1016/j.epsl.2016.08.025

Zhang, J., Gao, S., Ge, W., Wu, F., Yang, J., Wilde, S. A., et al. (2010). Geochronology of the Mesozoic volcanic rocks in the Great Xing'an Range, northeastern China: Implications for subduction-induced delamination. *Chemical Geology*, 276(3-4), 144–165. https://doi.org/10.1016/j.chemgeo.2010.05.013

Zhang, Q., Hu, S., Wang, L., Li, J., Dong, J., Wang, Y., et al. (2010). Formation and distribution of volcanic CO, gas pools in Songliao basin. *Acta Petrologica Sinica*, 26(1):109-120.

Zhang, R., Wu, Q., Sun, L., He, J., Gao, Z. (2014). Crustal and lithospheric structure of Northeast China from S-wave receiver functions. *Earth and Planetary Science Letters*, 401, 196–205. https://doi.org/10.1016/j.epsl.2014.06.017